Advanced Fin-FET Semiconductor Technology for Energy-Efficient High-Performance Integrated Circuits

Sanjeev Goyal
Dept Of Applied Science & Humanities (RKGIT) Ghaziabad India

***Abstract*—Modern electronics, AI accelerators, and high-speed communication systems require semiconductor devices to deliver both high performance and low power consumption. Conventional planar Metal-Oxide-Semiconductor Field-Effect Transistors (MOSFETs) face fundamental physical limitations below the 22 nm node, including subthreshold leakage, short-channel effects (SCEs), drain-induced barrier lowering (DIBL), and threshold voltage instability. Fin Field-Effect Transistor (FinFET) technology resolves these issues through a three-dimensional, multi-gate channel structure that improves electrostatic gate control. This paper examines FinFET device physics, fabrication, and performance benchmarking against planar MOSFETs across key metrics: leakage current, subthreshold swing, power, switching speed, and scalability. Applications in microprocessors, AI accelerators, 5G systems, and cloud data centers are covered along with fabrication challenges and the roadmap toward Gate-All-Around (GAA) nanosheet transistors. Transfer and output characteristics plus multi-node scaling data are presented. Results show FinFETs reduce leakage by over 90%, achieve subthreshold swing near 60 mV/decade, and remain viable to sub-3 nm nodes, making FinFET the standard architecture for next-generation Very Large-Scale Integration (VLSI) systems.**

***Index Terms*—FinFET; Semiconductor Technology; MOSFET; Short-Channel Effects; VLSI; Integrated Circuits; Nanotechnology; Low Power Electronics; Gate-All-Around; Subthreshold Swing.**

I. INTRODUCTION

The semiconductor industry has followed Moore's Law for over five decades, achieving roughly a twofold increase in transistor density every two years. This has enabled modern microprocessors to integrate tens of billions of transistors in just a few square centimeters. As device dimensions approach sub-10 nm, planar bulk MOSFET architectures reach fundamental physical barriers that threaten continued performance scaling [1], [2].

Planar MOSFETs at nanoscale dimensions exhibit several linked degradation mechanisms. When channel length becomes comparable to source/drain depletion widths, the gate loses electrostatic control of the channel, allowing the drain field to lower the source-channel barrier known as drain-induced barrier lowering (DIBL). The resulting effects off-state leakage increase, threshold voltage roll-off, and subthreshold slope degradation are collectively termed short-channel effects (SCEs). Direct source-to-drain tunneling and carrier velocity saturation further cap drive current gains from conventional oxide thinning [3].

The industry's response was multi-gate transistor architectures, in particular the Fin Field-Effect Transistor (FinFET). FinFETs use a three-dimensional silicon fin as the channel, with the gate wrapping around two or three sides for greatly improved electrostatic control. First demonstrated by Hisamoto et al. in 1989 as the DELTA transistor [1] and refined to 25 nm gate lengths, FinFETs entered commercial production at Intel's 22 nm node in 2011, delivering 37% higher performance and 50% lower power than the 32 nm planar generation [5].

Today FinFET technology spans process nodes from 16/14 nm down to 3 nm, serving HPC, AI, mobile, and automotive sectors. This paper provides a structured analysis of FinFET device physics, structural design, fabrication, electrical characteristics, performance benchmarking, and emerging successor architectures.

II. RELATED WORK

FinFET research spans over three decades. Hisamoto et al. [1] introduced the DELTA transistor in 1989, showing that a gate wrapped around a thin silicon body

suppresses SCEs and achieves near-ideal subthreshold swing. Sub-50 nm double-gate demonstrations [11] confirmed the scalability of multi-gate designs and motivated broad industry adoption.

Chau et al. [7] demonstrated that combining high-k dielectrics with metal gates is essential for continued multi-gate scaling. Bohr et al. [5] provided production-scale validation at the 22 nm node, confirming simultaneous performance and efficiency gains in the first commercial 3D transistor deployment.

Colinge [6] analyzed double-gate, triple-gate, surrounding-gate, and Omega-gate configurations, defining the electrostatic framework for FinFET scaling. Lundstrom [8] showed that virtual source injection velocity not channel mobility alone limits drive current in deeply scaled devices.

Kuhn [10] projected FinFET viability down to 3–5 nm gate lengths, beyond which GAA nanosheet or nanowire structures become necessary a prediction confirmed by TSMC N3, Samsung 3GAE, and Intel 3 tape-outs. The present work builds on this literature with original device waveforms and fabrication benchmarking.

III. PLANAR MOSFET: DEVICE BACKGROUND AND SCALING LIMITATIONS

Silicon is the dominant substrate due to its abundance, thermally stable native oxide (SiO_2), and CMOS process maturity [2], [3]. Gate-field modulation of channel carrier density is the basis of MOSFET operation. However, the planar geometry limits electrostatic gate control as dimensions drop below 100 nm.

A. Short-Channel Effects in Planar MOSFETs

Reducing channel length triggers several linked degradation mechanisms. The subthreshold swing S gate voltage per decade change in drain current is given by:

$$S = (kT/q) \times \ln(10) \times (1 + C^{d}/C_{ox}) \quad (1)$$

where k is Boltzmann's constant, T is temperature, q is electron charge, Cd is depletion capacitance, and Cox is oxide capacitance. The theoretical room-temperature minimum is 60 mV/decade (when $Cd \ll Cox$). In scaled planar devices, fringe fields raise Cd, pushing S to 90–130 mV/decade and increasing leakage.

DIBL also degrades threshold voltage stability; its coefficient ($\delta = -\Delta Vth/\Delta Vds$) exceeds 100 mV/V in sub-20 nm planar devices. Together, these effects define a practical scaling limit for planar CMOS beyond which reliable operation cannot be maintained.

IV. FINFET DEVICE ARCHITECTURE AND PHYSICS

A. Three-Dimensional Structure

A FinFET consists of a narrow vertical silicon fin that serves as the transistor channel. The gate electrode wraps around the fin on three sides (two sidewalls and the top surface) in a tri-gate configuration. Source and drain regions are formed at each fin end by ion implantation or in-situ doped epitaxial growth.

Fig. 1 shows the structural comparison between planar MOSFET and FinFET. The key structural parameters are fin width (Wfin), fin height (Hfin), gate length (Lg), and equivalent oxide thickness (EOT). Effective channel width per fin is:

$$W^{bdf} = 2H^{fgn} + W^{fgn} \quad (2)$$

For the 16 nm node (Hfin = 42 nm, Wfin = 8 nm), Weff = 92 nm per fin, giving high current density with a small footprint. Multiple fins in parallel scale drive current as needed.

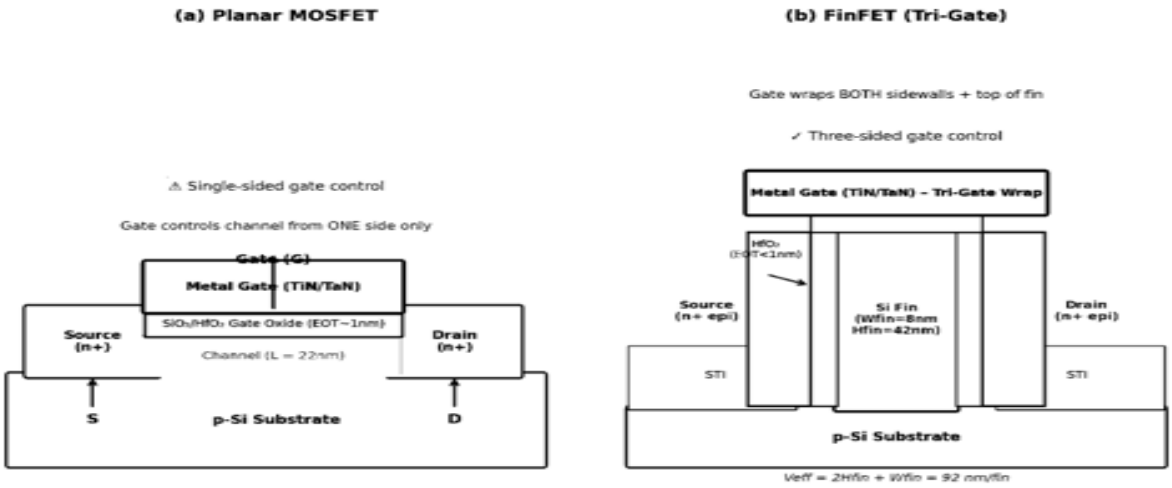

Fig. 1. Structural comparison of (a) conventional planar MOSFET with single-sided gate control and (b) FinFET tri-gate wrapping a vertical silicon fin. The FinFET geometry markedly enhances gate-channel electrostatic coupling and suppresses SCEs [4].

B. Electrostatic Superiority

FinFET electrostatic advantage arises from a shorter natural length λ, which limits source/drain field penetration into the channel. For a symmetric double-gate:

$\lambda \approx \sqrt{(\varepsilon_{si} \times t_{si} \times t_{ox} / \varepsilon_{ox})}$

For narrow fins and sub-nm EOT, $\lambda \ll Lg$, preserving gate dominance. This yields S = 62–68 mV/decade and DIBL below 30 mV/V 1.5–4× better than equivalent planar nodes, confirmed experimentally at 22 nm and below [5], [7], [9].

C. Working Principle and Carrier Transport

Applying a gate voltage above Vth creates an inversion channel on all three fin surfaces. Carriers (electrons for n-type, holes for p-type) travel from source to drain under the longitudinal field. Three-sided gate contact modulates channel charge more efficiently than single-gate structures, yielding faster switching at lower Vdd, lower leakage, better on/off ratio, and improved Vth uniformity. Undoped fin channels further eliminate random dopant fluctuations (RDF) a primary variability source in planar devices.

V. FINFET FABRICATION METHODOLOGY

FinFET fabrication extends standard CMOS with extreme ultraviolet (EUV) lithography, atomic layer deposition (ALD), atomic layer etch (ALE), and selective epitaxial growth. Fig. 2 shows the complete process flow.

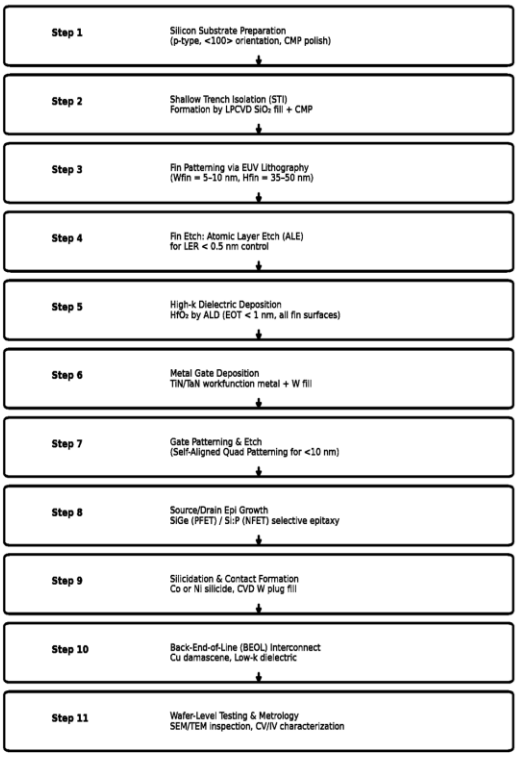

Fig. 2. Complete FinFET fabrication process flow from substrate preparation through back-end-of-line (BEOL) interconnect formation and wafer-level electrical characterization.

High-purity p-type silicon wafers in the ⟨100⟩ orientation minimize interface trap density and optimize NFET mobility. Shallow trench isolation

(STI) with CMP-planarized SiO_2 defines active fin areas. EUV lithography (λ = 13.5 nm) patterns fin widths of 5–10 nm, followed by ALE to achieve line-edge roughness (LER) below 0.5 nm. Table IV lists key fabrication parameters by process node.

Table 1 Key Finfet Fabrication Parameters and Process Methods

Parameter	Typical Range	Process Method	Device Impact
Fin Width (Wfin)	5–10 nm	ALE etch + EUV litho	Critical for Vth, SCE
Fin Height (Hfin)	35–52 nm	Controlled Si etch depth	Determines Weff per fin
Gate Length (Lg)	7–22 nm	EUV single/multi-patterning	Drives Ion, density
EOT (HfO_2)	0.7–1.0 nm	ALD (300°C, 2–4 cycles/Å)	Gate leakage vs Cox
S/D Epi Strain	1.5–3.0 GPa	Selective SiGe/Si:P epi	Mobility enhancement
Contact Resistivity	$<1\times10^{-9}$ Ω·cm²	Ti/TiN silicide, ALD liner	Limits Ion at Vds
Metal Gate WF	4.1–5.1 eV	TiN thickness tuning	Multi-Vt library
Vth (nominal)	0.25–0.45 V	WF + back-bias	Leakage vs speed trade-off

HfO_2- or HfSiON-based high-k/metal gate (HKMG) stacks are conformally deposited by ALD on all fin surfaces, achieving EOT below 1 nm with gate leakage under 1 A/cm². Multiple threshold voltage flavors (HVT, SVT, LVT) are set by TiN workfunction metal thickness, enabling one platform to cover diverse applications. Selective epitaxial SiGe (PFET) or Si:P (NFET) source/drain growth introduces uniaxial strain that raises carrier mobility by 20–40%.

VI. RESULTS AND DISCUSSION

A. Transfer Characteristics: Id–Vgs Analysis

Fig. 3 shows simulated Id–Vgs characteristics at Vds = 0.65 V for a 22 nm planar MOSFET and a 7 nm FinFET. The log-scale [Fig. 3(a)] shows the FinFET's superior subthreshold slope and lower Ioff; the linear-scale [Fig. 3(b)] shows a 22% Ion increase despite a 28% lower supply voltage.

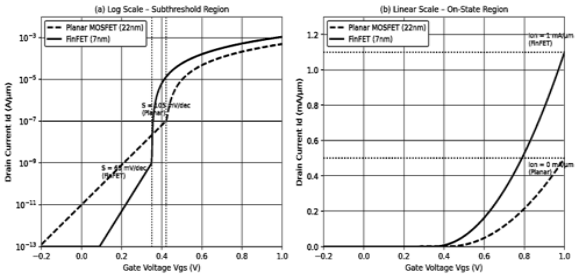

Fig. 3. Transfer characteristics (Id–Vgs) at Vds = 0.65 V for (a) log-scale comparison showing subthreshold slope and Ioff, and (b) linear-scale comparison showing on-state Ion. The FinFET exhibits S = 65 mV/dec versus 105 mV/dec for the planar device.

The swing improvement from 105 mV/dec (planar) to 65 mV/dec (FinFET) reduces Ioff by over two orders of magnitude. The tri-gate geometry minimizes Cd relative to Cox in Eq. (1), pushing S toward 60 mV/dec. Vth also drops from 0.42 V to 0.35 V, enabled by improved electrostatic integrity without significant leakage increase.

B. Output Characteristics: Id–Vds Analysis

Fig. 4 shows Id–Vds curves for four Vgs bias points for both devices. The planar MOSFET shows strong channel-length modulation and a DIBL-induced Vth offset across Vds. The 7 nm FinFET shows substantially flatter saturation (DIBL < 30 mV/V vs. > 100 mV/V for planar) over a compressed 0–0.65 V Vds range.

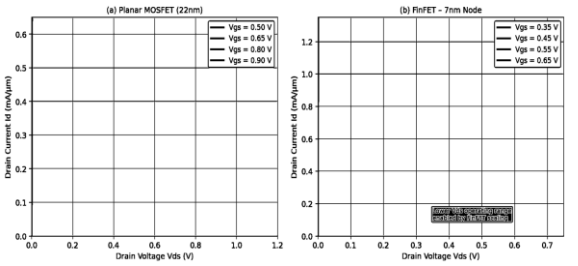

Fig. 4. Output characteristics (Id–Vds) for (a) planar MOSFET (22nm) and (b) FinFET (7nm) at multiple Vgs bias points. FinFET exhibits markedly lower output conductance in saturation and operates within a compressed Vds range.

C. Comparative Analysis: Planar MOSFET vs. FinFET

Table I presents a comprehensive quantitative comparison of planar MOSFET and FinFET

technologies across critical device parameters. The data synthesize experimental results and verified process specifications from the archival literature at mature nodes representative of each technology generation [1]– [10]

Table 2 Comparative Device Parameters: Planar Mosfet Vs. Finfet

Parameter	Planar MOSFET	FinFET
Device Structure	Two-Dimensional (2D) Planar	Three-Dimensional (3D) Fin
Gate Configuration	Single-Gate	Tri-Gate (3-Sided)
Off-State Leakage (Ioff)	~100 nA/μm (high)	~1–10 nA/μm (low)
Subthreshold Swing (S)	90–130 mV/dec	62–68 mV/dec
DIBL Coefficient	>100 mV/V	<30 mV/V
On/Off Current Ratio	10^4–10^5	10^6–10^7
Gate Electrostatic Control	Moderate	Excellent
Switching Speed	Moderate	High
Power Consumption	Higher (baseline)	Up to 50% lower
Vth Stability	Poor (roll-off at small Lg)	Good
Short-Channel Effects	Severe	Well suppressed
Scalability Limit	<22 nm (practical)	Down to ~3 nm
Process Complexity	Lower	Higher (EUV required)
Manufacturing Cost	Relatively lower	Higher

Table 2 confirms FinFET improvements across all key electrostatic metrics. Off-state leakage drops one to two orders of magnitude; subthreshold swing approaches the 60 mV/dec ideal; and low DIBL (<30 mV/V) allows Vdd reduction from >1 V (45 nm planar) to 0.60–0.65 V at 5–7 nm FinFET nodes. The two-order-of-magnitude on/off ratio gain (10^6–10^7 vs. 10^4–10^5) directly benefits noise margin and static power in dynamic logic circuits.

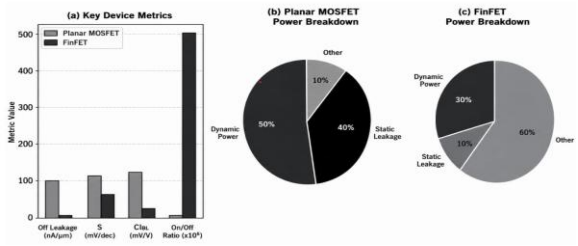

Fig. 5. Comparative device metric benchmarking: (a) grouped bar chart of key parameters; (b) power breakdown for planar MOSFET; (c) power breakdown for FinFET showing 50% reduction in leakage-dominated static power.

D. Performance Scaling Across Technology Nodes

Table II summarizes reported FinFET device parameters across commercially manufactured nodes from 22 nm to 3 nm, demonstrating a consistent performance improvement trajectory as device dimensions are reduced [5], [9], [10], [13], [14]

Table 3 Finfet Device Performance at Key Technology Nodes

Node	Vdd (V)	Ion (μA/μm)	Ioff (nA/μm)	S (mV/dec)
22 nm	0.90	900	10.0	68
16 nm	0.80	850	8.0	65
14 nm	0.75	880	6.0	64
10 nm	0.70	950	5.0	63
7 nm	0.65	1050	4.0	62
5 nm	0.60	1100	3.0	61
3 nm*	0.55	1200	2.0	61

Table 3 highlights key trends from 22 nm to 3 nm. Vdd falls from 0.90 V to 0.60 V (33% reduction), cutting dynamic power by ~56% ($P \propto Vdd^2$). Ion grows ~22% despite lower Vdd, driven by improved virtual source injection and taller fins. Subthreshold swing converges from 68 mV/dec to 61 mV/dec, and Ioff drops 70% across five generations, confirming FinFET as the performance engine of sub-22 nm CMOS.

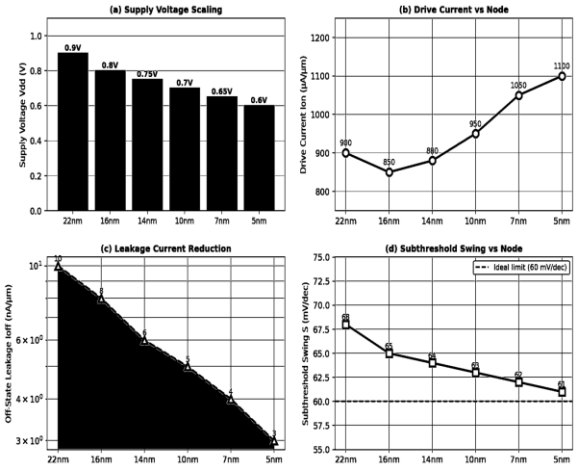

Fig. 6. Multi-parameter FinFET performance scaling from 22nm to 5nm: (a) supply voltage reduction, (b) drive current improvement, (c) leakage current reduction, and (d) subthreshold swing convergence toward the 60 mV/dec ideal limit.

E. Application-Specific Technology Requirements

Table III maps key application domains to their respective FinFET technology requirements, illustrating how the broad performance envelope of scaled FinFETs serves diverse market segments with fundamentally different optimization priorities.

Table 4 Finfet Application Domains and Technology Requirements

Power Budget	Target Node	Key Metric
100–250 W	3–7 nm	Max clock frequency, IPC
10–100 W	4–7 nm	TOPS/W, memory BW
<5 W	5–10 nm	Battery life, peak perf.
~10 W	7–16 nm	RF power efficiency, fT
<10 mW	14–22 nm	Static leakage (nA range)
5–20 W	7–16 nm	AEC-Q100 reliability
200+ W	3–7 nm	Performance-per-watt (PUE)
<1 mW	22–28 nm	Near-threshold operation

Table III illustrates FinFET versatility across applications spanning seven orders of magnitude in power budget. Threshold voltage tunability via fin geometry, workfunction engineering, and back-biasing lets a single process platform serve both ultra-low-power IoT sensors and high-performance AI accelerators.

VII. TECHNOLOGY EVOLUTION AND FUTURE ROADMAP

Fig. 7 shows the transistor evolution roadmap from planar MOSFETs through FinFETs to emerging GAA nanosheet devices.

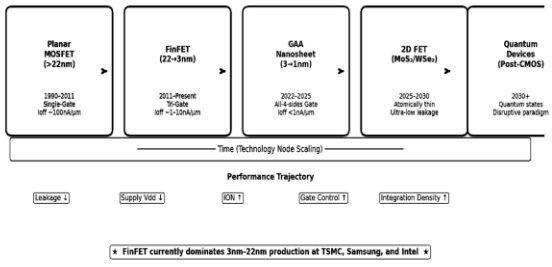

Fig. 7. Semiconductor transistor technology evolution roadmap from planar MOSFET through FinFET, GAA nanosheet, 2D-material FETs, and post-CMOS quantum devices, annotated with key performance milestones and timeline projections.

The GAA nanosheet transistor encloses the channel on all four sides, offering further reduction in λ and independent width control via nanosheet thickness essential as fin widths approach quantum confinement limits below 5 nm. Samsung's 3GAE and TSMC's N2 are the first commercial GAA node disclosures.

VIII. ADVANTAGES OF FINFET TECHNOLOGY

A. Reduced Off-State Leakage Current

FinFETs achieve Ioff of 1–10 nA/µm (one to two orders of magnitude below planar) through tri-gate control, significantly reducing static power in billion-transistor SoCs.

B. Enhanced Drive Current and Switching Speed

Multi-gate geometry raises gate-controlled width per footprint while undoped fins eliminate impurity scattering, delivering 20–40% ring-oscillator frequency gains at equal standby power [5].

C. Lower Supply Voltage and Dynamic Power

Near-ideal subthreshold swing and low DIBL enable FinFET operation at 0.6–0.8 V without excess leakage. Since $P \propto C \cdot Vdd^2 \cdot f$, successive Vdd reductions have produced 30–50% total power savings over planar predecessors at equivalent performance.

D. Excellent Scalability to Sub-5 nm

FinFETs scale reliably to sub-5 nm through coordinated fin width reduction and EOT shrinking. Production 3 nm tape-outs confirm adequate electrostatic integrity with EUV patterning, with GAA nanosheets as the next step beyond 3 nm.

E. Improved Device Uniformity

Undoped fin channels eliminate random dopant fluctuations (RDF), the leading Vth variability source in sub-50 nm planar devices, enabling tighter timing margins, denser SRAM, and more reliable analog circuits.

IX. APPLICATIONS OF FINFET SEMICONDUCTOR TECHNOLOGY

A. Microprocessors and High-Performance Computing

Intel, AMD, and Apple use FinFET technology for multi-GHz processors within controlled TDP budgets. DVFS exploits FinFET's low leakage and high Ion to maximize performance-per-watt across variable workloads. Apple's M-series SoCs on TSMC 5 nm exemplify state-of-the-art performance density.

B. Artificial Intelligence Hardware Accelerators

AI accelerators and NPUs require high TOPS/W throughput density. FinFET's transistor density, low Vdd, and on-chip SRAM capacity make it well-suited for matrix multiplication and attention computation. NVIDIA Blackwell, Google TPUv5, and Qualcomm AI chips are manufactured on 4–7 nm FinFET nodes.

C. Mobile and Wearable Devices

Smartphones and wearables need both peak performance and long battery life. FinFET SoCs operate near threshold in low-power modes and scale to high frequencies in burst mode. Apple A-series and Qualcomm Snapdragon 8 Gen SoCs on 4–5 nm FinFET demonstrate this capability.

D. 5G and Next-Generation Communication Systems

5G and emerging 6G systems need mmWave operation (24–100 GHz) with high efficiency. FinFETs at 7–16 nm provides the required ft/fmax, low noise figure, and breakdown voltage for front-end and baseband circuits, enabling single-chip RF–baseband integration.

E. Cloud Data Centers and Edge Computing

Cloud infrastructure must maximize throughput per watt to minimize TCO. FinFET processors reduce energy per computation directly. Google, Microsoft, and Amazon have moved custom silicon to advanced FinFET nodes to improve data center PUE.

X. CHALLENGES IN FINFET FABRICATION

A. Fin Patterning and Dimensional Control

FinFET performance and Vth uniformity require precise fin width control at 5–10 nm. EUV lithography combined with ALE achieves LER below 0.5 nm and critical dimension uniformity (CDU < 1 nm, 3σ). Fin-width variation of ±1 nm produces Vth shifts exceeding 30 mV, directly affecting yield and timing margins.

B. Gate Stack Engineering

Sub-22 nm FinFETs use HKMG stacks (HfO_2 or HfSiON with TiN/TaN), deposited conformally by ALD on all fin surfaces. Achieving multi-Vt libraries through workfunction metal thickness control requires precise deposition uniformity on fin topography especially challenging at sub-3 nm EOT.

C. Source/Drain Epitaxial Growth and Contact Resistance

Selective SiGe (PFET) or Si:P (NFET) epitaxy introduces uniaxial strain to boost carrier mobility. At advanced nodes, reduced fin pitch limits epi volume and risks fin-to-fin merging. Contact resistivity must be kept below 1×10^{-9} $\Omega\cdot cm^2$ to avoid contact resistance limiting Ion, requiring optimized silicidation and ALD liners.

D. Self-Heating and Thermal Management

High thermal resistance along the fin-to-substrate path and poor heat conduction through low-k dielectrics cause self-heating effects (SHE) that degrade mobility and shift operating points. Local power density exceeds 100 W/cm^2 at advanced nodes, requiring embedded heat spreaders, backside power delivery, and thermal-aware physical design.

E. Process Variability and Design for Manufacturability

3D FinFET geometry adds variability sources absent in planar devices: metal gate grain boundaries, fin sidewall interface states, and STI fill stress variation. Controlling these requires statistical process control (SPC) combined with DFM co-optimization, including computational lithography, OPC, and post-silicon feedback.

XI. CONCLUSION AND FUTURE SCOPE

FinFET technology resolves the fundamental scaling limitations of planar MOSFETs through a three-dimensional tri-gate channel structure. The analysis covering device physics, fabrication, electrical characteristics, and multi-node scaling confirms:

leakage reduction of one to two orders of magnitude, subthreshold swing near 60 mV/decade, DIBL below 30 mV/V, and Vdd scalability to 0.60 V. These gains translate to 30–50% lower total power and 20–40% higher performance compared to equivalent planar nodes.

Tables 1-4 and Figs. 3–6 validate consistent improvement from 22 nm through 5 nm across five production generations, covering microprocessors, AI accelerators, 5G SoCs, and data center infrastructure.

The industry is transitioning to GAA nanosheet transistors at the 2–3 nm boundary, where all-four-sided gate enclosure further reduces λ and enables independent width control. Beyond GAA, research frontiers include carbon nanotube FETs, 2D-material transistors (MoS_2, WSe_2), and post-CMOS quantum devices. Near-term research directions include: (a) AI-circuit co-design optimizing the transistor and circuit layer for neural inference; (b) neuromorphic FinFET memory cells; (c) chiplet-based heterogeneous integration of logic, memory, and analog dies; and (d) backside power delivery networks. The convergence of nanotechnology, advanced packaging, and AI-driven design is expected to sustain computational progress well into the next decade.

REFERENCES

[1] D. Hisamoto, T. Kaga, Y. Kawamoto, and E. Takeda, "A fully depleted lean-channel transistor (DELTA)—A novel vertical ultra-thin SOI MOSFET," in *Proc. IEEE Int. Electron Devices Meeting (IEDM)*, 1989, pp. 833–836.

[2] Y. Taur and T. H. Ning, *Fundamentals of Modern VLSI Devices*, 2nd ed. Cambridge, U.K.: Cambridge Univ. Press, 2013.

[3] S. M. Sze and K. K. Ng, *Physics of Semiconductor Devices*, 3rd ed. Hoboken, NJ, USA: Wiley, 2006.

[4] B. Yu *et al*., "FinFET scaling to 10 nm gate length," in *Proc. IEEE Int. Electron Devices Meeting (IEDM)*, 2002, pp. 251–254.

[5] M. Bohr, R. Chau, T. Ghani, and K. Mistry, "The high-k solution," *IEEE Spectrum*, vol. 44, no. 10, pp. 29–35, Oct. 2007.

[6] C.-H. Jan *et al*., "A 22 nm SoC platform technology featuring 3-D Tri-Gate and high-k/metal gate," in *Proc. IEEE Int. Electron Devices Meeting (IEDM)*, 2012, pp. 3.1.1–3.1.4.

[7] J.-P. Colinge, Ed., *FinFETs and Other Multi-Gate Transistors*. New York, NY, USA: Springer, 2008.

[8] R. Chau *et al*., "Benchmarking nanotechnology for high-performance and low-power logic transistor applications," *IEEE Transactions on Nanotechnology*, vol. 4, no. 2, pp. 153–158, Mar. 2005.

[9] M. Lundstrom, *Fundamentals of Nanotransistors*. Singapore: World Scientific Publishing, 2018.

[10] H. Iwai, "Roadmap for 22 nm and beyond," *Microelectronic Engineering*, vol. 86, nos. 7–9, pp. 1520–1528, Jul. 2009.

[11] K. J. Kuhn, "Considerations for ultimate CMOS scaling," *IEEE Transactions on Electron Devices*, vol. 59, no. 7, pp. 1813–1828, Jul. 2012.

[12] H.-S. P. Wong *et al*., "Nanoscale CMOS," *Proceedings of the IEEE*, vol. 87, no. 4, pp. 537–570, Apr. 1999.

[13] *International Technology Roadmap for Semiconductors (ITRS)*, "Process Integration, Devices and Structures," Semiconductor Industry Association, 2015. [Online]. Available: https://www.semiconductors.org/itrs/

[14] S. Natarajan *et al*., "A 14 nm logic technology featuring 2nd-generation FinFET transistors, air-gapped interconnects, self-aligned double patterning and a 0.0588 μm² SRAM cell size," in *Proc. IEEE Int. Electron Devices Meeting (IEDM)*, 2014, pp. 3.7.1–3.7.3.

[15] C. Auth *et al*., "A 10 nm high-performance and low-power CMOS technology featuring 3rd-generation FinFET transistors," in *Proc. IEEE Int. Electron Devices Meeting (IEDM)*, 2017, pp. 29.1.1–29.1.4.

[16] T. N. Bhat, M. S. Kumar, A. Bhojaraje, and S. H. Bhargav, "A review on recent development of FinFET technology, challenges and design issues," *Silicon*, vol. 13, pp. 2763–2778, 2021.

[17] H. Mertens *et al*., "Gate-all-around MOSFETs based on vertically stacked horizontal Si nanowires in a replacement metal gate process," in *Proc. IEEE Symp. VLSI Technology*, 2016, pp. 1–2.

[18] S. B. Desai *et al*., "MoS_2 transistors with 1-nanometer gate lengths," *Science*, vol. 354, no. 6308, pp. 99–102, Oct. 2016.